



# Massless charged wormhole solution in Einstein–Maxwell–Scalar theory

S. Habib Mazharimousavi<sup>a</sup>

Department of Physics, Faculty of Arts and Sciences, Eastern Mediterranean University, North Cyprus via Mersin 10, Famagusta, Turkey

Received: 23 December 2021 / Accepted: 9 March 2022  
© The Author(s) 2022

**Abstract** A new exact wormhole solution in Einstein–Maxwell–Scalar theory is introduced. The wormhole solution is accompanied by a non-black hole naked singular branch solution. Both of the solutions are massless such that with charge zero the spacetime coincides with the vacuum Minkowski flat spacetime. In addition to that, the wormhole solution seems to be the missing part of the class of solutions in the standard Einstein–Maxwell–Dilaton theory with an arbitrary dilaton parameter.

## 1 Introduction

In 1916, it was Ludwig Flamm who realized that the Schwarzschild solution may represent a wormhole [1]. This was almost immediately after Schwarzschild published his solution [2]. In 1935 Einstein and Rosen introduced the so-called Einstein–Rosen bridge which is a non-traversable wormhole [3]. Furthermore, the notion of a traversable wormhole was developed in the pioneering paper of Morris and Thorne [4]. More details on the traversable wormholes can be found in the book of Visser [5]. Wormhole solutions have been studied in different theories of gravity. For instance, Lobo and Oliveira constructed traversable wormhole in  $f(R)$  theories of gravity in [6] (see also [7]), and very recently Banergee et al. investigated the existence of wormhole geometries in  $f(Q)$  theory of gravity, where  $Q$  is the non-metricity scalar [8]. A comprehensive review paper on traversable wormholes has been recently published by Lobo in [9].

On the other hand, it is well-known that the low energy limit of the string theory yields the action of Einstein’s gravity coupled with other fields such as dilaton and axion [10]. Coupling of dilaton to the gauge fields changes physical properties of the charged black hole such as the causal structure and the thermodynamic properties [11–18]. The first such solu-

tion i.e., black hole solution in Einstein–Maxwell–Dilaton (EMD) theory was introduced by Gibbons in 1982 [19]. However, the first static spherically symmetric solution in gravity coupled with massless scalar field was studied by Fisher in 1948 [20]. There are several exact solutions in EMD theory [21–26] as well as Einstein–Maxwell–Scalar (EMS) [27–36] theory in the literature. In particular, one of the early work which focusses on wormhole solution in dilatonic theory is [37]. In [37] the authors give comprehensive information on the construction of the complete wormhole solution the emergence of the two asymptotic regimes and how to implement any necessary distribution of matter for the smooth matching of the two spacelike regimes. In addition to that, the spherically symmetric EMS theory with the scalar field coupled nonminimally to Maxwell’s invariance via a general coupling function has been discussed comprehensively in [38]. In [38], the coupling function is classified as of *Class I or dilatonic-type* and *Class II or scalarised-type*. In *Class I* the coupling function  $W(\phi)$  (in Eq. (2) below) satisfies  $\left. \frac{dW(\phi)}{d\phi} \right|_{\phi=0} \neq 0$  and  $\phi(r) = 0$  doesn’t solve the field equations and consequently the Reissner–Nordström black hole is not a solution for the field equations (Eqs. (5)–(7) below). The well-known  $W(\phi) = e^{\alpha\phi}$  belongs to this class. On the other hand, in *Class II* the coupling function satisfies  $\left. \frac{dW(\phi)}{d\phi} \right|_{\phi=0} = 0$  and consequently  $\phi(r) = 0$  solves the field equations with the Reissner–Nordström as of its solution. There are two subclasses named as *Subclass IIA or scalarised-connected-type* where  $\left. \frac{d^2W(\phi)}{d\phi^2} \right|_{\phi=0} \neq 0$  and *Subclass IIB or scalarised-disconnected-type* where  $\left. \frac{d^2W(\phi)}{d\phi^2} \right|_{\phi=0} = 0$ . In subclass *IIA* the black hole solution bifurcate from Reissner–Nordström such that in the limit  $\phi \rightarrow 0$  it coincides with RN. Also, it may be associated with the so-called tachyonic instability against the scalar perturbation. One example of this class can be  $W(\phi) = e^{\alpha\phi^2}$ . In subclass *IIB*, the black hole solution does not bifurcate from RN and therefore at the limit  $\phi \rightarrow 0$ , it

<sup>a</sup>e-mail: [habib.mazhari@emu.edu.tr](mailto:habib.mazhari@emu.edu.tr) (corresponding author)

doesn't reduce to RN solution. Due to  $\left. \frac{d^2 W(\phi)}{d\phi^2} \right|_{\phi=0} = 0$  there is no tachyonic instability in this subclass and as an example is  $W(\phi) = 1 + \alpha\phi^4$ .

With respect to this classification and the comprehensive study in Ref. [38], here in this work, we aim to introduce a wormhole solution that belongs to the *Subclass IIA or scalarised-connected-type* models. We should add that scalarized wormholes have been considered in the literature. One of the recent works was published by Ibadov et al. in [39] where the phenomenon of scalarization and the interesting features of scalarized compact objects have been discussed. In summary, scalarization takes place when the scalar field  $\phi$  couples with gravity through a source term  $\mathcal{I}$ . The source term  $\mathcal{I}$  in Eq. (1) (below) is the electromagnetic invariant i.e.,  $\mathcal{I} = -F_{\mu\nu}F^{\mu\nu}$  however in general it can be a topological invariant too such as the Gauss–Bonnet and the Chern–Simons invariants (in 3 + 1-dimensions) given by  $\mathcal{I} = R_{GB}^2 = R^2 - 4R_{\mu\nu}R^{\mu\nu} + R_{\mu\nu\rho\sigma}R^{\mu\nu\rho\sigma}$  and  $\mathcal{I} = R_{CS}^2 = \frac{1}{2\sqrt{-g}}\epsilon^{\rho\gamma\sigma\tau}R^{\mu}_{\nu\kappa\lambda}R^{\nu}_{\mu\rho\sigma}$ , respectively. The resultant theory are called the Einstein–Scalar–Gauss–Bonnet [40–43] and the Einstein–Scalar–Chern–Simons [44–46], respectively. As we mentioned above, the interesting phenomenon of the spontaneous scalarization occurs when  $\left. \frac{dW(\phi)}{d\phi} \right|_{\phi=0} \neq 0$  and  $\phi = 0$  doesn't solve the field equations. For more information and references we refer to the introduction of [39].

This paper is organized as follows. In Sect. 2 we introduce the action and the field equations. In Sect. 3 we find the solutions to the field equations. In the same section, we investigate the two distinct solutions with details. We summarize and conclude the paper in Sect. 4.

## 2 The action and field equations

We start with the action ( $16\pi G = c = 1$ )

$$I = \int \sqrt{-g} [\mathcal{R} - 2\partial_\mu\phi\partial^\mu\phi - W_S(\phi)F_{\mu\nu}F^{\mu\nu}] d^4x \quad (1)$$

in which  $\mathcal{R}$  is the Ricci scalar,  $F_{\mu\nu} = \partial_\mu A_\nu - \partial_\nu A_\mu$  is the Maxwell gauged field,  $\phi$  is the scalar field, and

$$W_S(\phi) = \frac{16}{\phi^4 - 4\phi^2 + 16} \quad (2)$$

is the coupling function satisfying

$$\left. \frac{dW_S(\phi)}{d\phi} \right|_{\phi=0} = 0 \quad (3)$$

and

$$\left. \frac{d^2W_S(\phi)}{d\phi^2} \right|_{\phi=0} = \frac{1}{2} \neq 0. \quad (4)$$

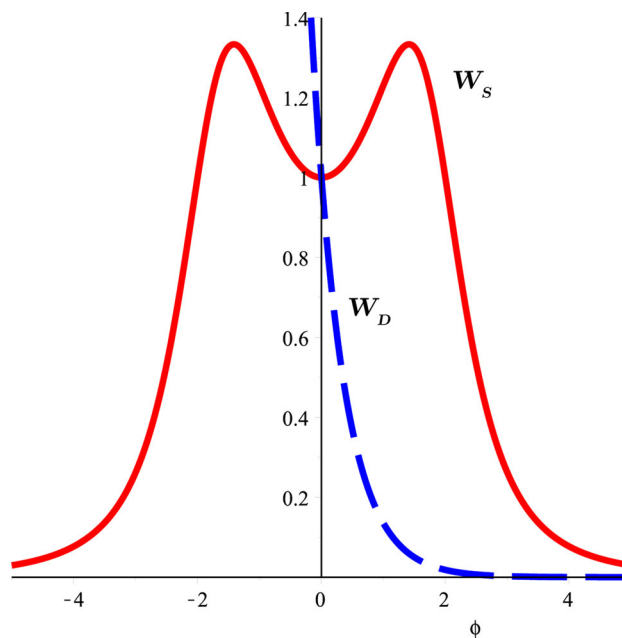


**Fig. 1** Plots of  $e^{-2\phi}$  (blue-dash) and  $\frac{16}{\phi^4 - 4\phi^2 + 16}$  (red-solid) with respect to  $\phi$ . The later one admits two maximum and one minimum (vacuum states)

Hence,  $W_S(\phi)$  belongs to *Subclass IIA or scalarised-connected-type* of Ref. [38]. As it is depicted in Fig. 1, where the standard dilaton potential  $W_D(\phi) = e^{-2\alpha\phi}$  is plotted with  $\alpha = 1$  together with  $W_S(\phi) = \frac{16}{\phi^4 - 4\phi^2 + 16}$ , while  $W_D(\phi)$  admits a monotonic decreasing function,  $W_S(\phi)$  asymptotically goes to zero and admits two maximum and one local minimum (vacuum states) in a new form of the Mexican hat.

Variation of the action with respect to the metric tensor  $g_{\mu\nu}$ , Maxwell gauge potential  $A_\mu$  and the scalar field  $\phi$  gives the field equations given by

$$R^\nu_\mu = 2\partial_\mu\phi\partial^\nu\phi + \frac{W_S(\phi)}{2}(4F_{\mu\lambda}F^{\nu\lambda} - F_{\alpha\beta}F^{\alpha\beta}\delta^\nu_\mu), \quad (5)$$

$$\nabla_\mu(W_S(\phi)F^{\mu\nu}) = 0 \quad (6)$$

and

$$\nabla_\mu(\partial^\mu\phi) = \frac{1}{4}\frac{dW_S(\phi)}{d\phi}F_{\mu\nu}F^{\mu\nu}, \quad (7)$$

respectively. Our static spherically symmetric line element is chosen to be

$$ds^2 = -f(r)dt^2 + \frac{1}{f(r)}dr^2 + R(r)^2 d\Omega^2 \quad (8)$$

and the Maxwell field is a radial electric field

$$\mathbf{F} = \frac{1}{2}F_{\mu\nu}dx^\mu \wedge dx^\nu = E(r)dt \wedge dr \quad (9)$$

which is produced by an electric monopole. Here in (8) and (9)  $f(r)$ ,  $R(r)$  and  $E(r)$  are unknown to be found.

### 3 The solution

The field equations explicitly become

$$R_t^t = \frac{1}{2} W_S(\phi) F_{\alpha\beta} F^{\alpha\beta}, \tag{10}$$

$$R_r^r = 2f(r)\phi'(r)^2 + \frac{1}{2} W_S(\phi) F_{\alpha\beta} F^{\alpha\beta}, \tag{11}$$

$$R_\theta^\theta = R_\varphi^\varphi = -\frac{W_S(\phi)}{2} F_{\alpha\beta} F^{\alpha\beta}, \tag{12}$$

$$E = \frac{q}{R^2 W_S(\phi)} \tag{13}$$

and

$$(R^2 f \phi')' = \frac{R^2}{4} \frac{dW_S(\phi)}{d\phi} F_{\alpha\beta} F^{\alpha\beta}, \tag{14}$$

where  $F_{\alpha\beta} F^{\alpha\beta} = -2E^2$ . Combining the first two equations yields

$$R_r^r - R_t^t = 2f(r)\phi'(r)^2 \tag{15}$$

and combining the first and the third equations implies

$$R_t^t + R_\theta^\theta = 0. \tag{16}$$

Knowing that,

$$R_t^t = -\frac{1}{2R^2} (R^2 f')' \tag{17}$$

$$R_r^r = R_t^t - 2f \frac{R''}{R} \tag{18}$$

and

$$R_\theta^\theta = R_\varphi^\varphi = -\frac{1}{2R^2} \left( (R^2 f')' - 2 \right), \tag{19}$$

(16) becomes

$$(R^2 f)'' = 2 \tag{20}$$

or simply

$$f(r) = \frac{(r+r_1)(r+r_2)}{R^2} \tag{21}$$

in which  $r_1$  and  $r_2$  are two integration constants. Furthermore, (15) reduces to

$$\frac{R''}{R} = -\phi'(r)^2. \tag{22}$$

In summary, we are left only with (10) and (14) which explicitly read

$$(R^2 f')' = 2 \frac{q^2}{R^2 W_S} \tag{23}$$

and

$$(R^2 f \phi')' = -\frac{1}{2} \frac{dW_S}{d\phi} \frac{q^2}{R^2 W_S^2} \tag{24}$$

and (22) while the metric function is given by (21). Moreover, considering  $\frac{dW_S}{d\phi} = \frac{W_S'}{\phi'}$  in (24) where the prime stands for the derivative with respect to  $r$ , and Eqs. (21) and (22), after a rather tedious manipulation one can show that, irrespective of the form of  $W_S$ , these two equations (i.e, Eq.s (23) and (24)) are simultaneously satisfied. This in turn implies that the number of independent differential equations reduces to only two equations, i.e., (22) and (23). Finally, with the explicit form of  $W_S$  given in Eq. (2), the solutions of the field equations are found to be

$$f_\pm(r) = \left(1 \pm \frac{|q|}{r}\right)^2 \frac{1}{\ln^2\left(1 \pm \frac{|q|}{r}\right)}, \tag{25}$$

$$R_\pm(r) = r \ln\left(1 \pm \frac{|q|}{r}\right), \tag{26}$$

$$\exp\left(\frac{\phi_\pm^2}{4}\right) = \left(1 \pm \frac{|q|}{r}\right) \tag{27}$$

and

$$E_\pm(r) = \frac{|q|}{r^2} \left( \ln\left(1 \pm \frac{|q|}{r}\right) - 1 + \frac{1}{\left(1 \pm \frac{|q|}{r}\right)} \right). \tag{28}$$

We should add that the integration constants have been set in a manner that both equations i.e., (22) and (23) have been satisfied. In Figs. 2 and 3 we plotted  $f_\pm(r)$  in terms of  $r$  for  $|q| \in [0.1, 3]$  with equal steps.

Both solution are asymptotically non-flat and  $f_+(r)$  admits a singularity at  $r = 0$ . Furthermore, for large  $r$  we

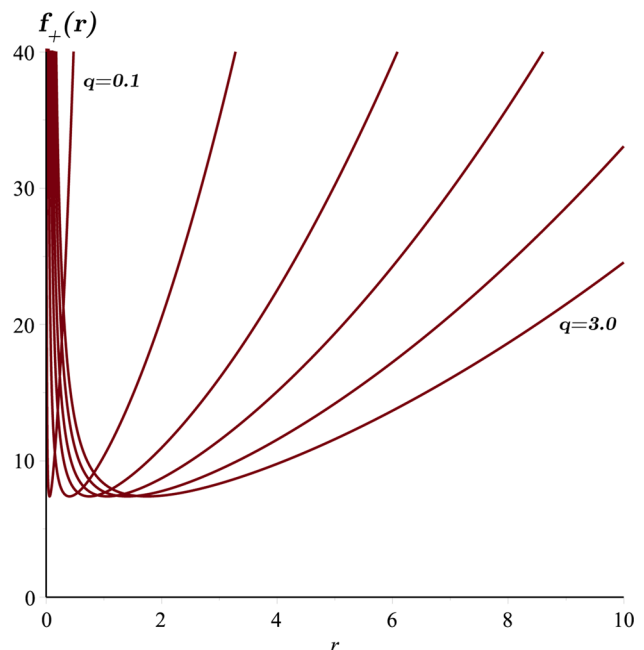


**Fig. 2** Plot of  $f_+(r)$  in terms of  $r$  for various values of  $q = 0.1 \dots 3.0$  with equal steps

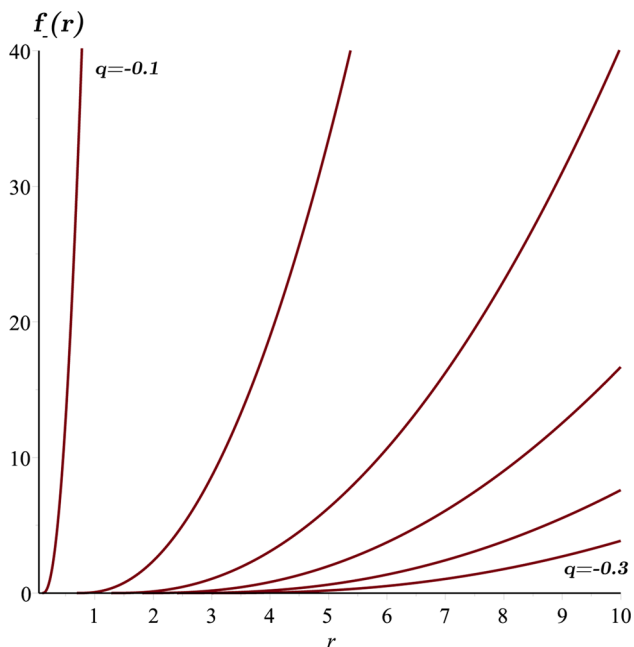


**Fig. 3** Plot of  $f_-(r)$  in terms of  $r$  for various values of  $|q| = 0.1 \dots 3.0$  with equal steps

obtain

$$\lim_{r \rightarrow \infty} f_{\pm}(r) = \frac{37}{12} \pm \frac{3}{|q|}r + \frac{1}{q^2}r^2 - \frac{7|q|}{6r} + O\left(\frac{1}{r^2}\right) \sim \frac{1}{q^2}r^2 \quad (29)$$

and

$$\lim_{r \rightarrow \infty} R_{\pm}(r) = \pm |q| - \frac{q^2}{r} + O\left(\frac{1}{r^2}\right) \sim \pm |q|. \quad (30)$$

Therefore the large  $r$  behavior of the solution is approximately expressed by

$$ds_{\pm}^2 \sim -\frac{r^2}{q^2}dt^2 + \frac{q^2}{r^2}dr^2 + q^2d\Omega^2 \quad (31)$$

which is nothing but the charged Bertotti–Robinson (BR) spacetime [47–49]. To see this explicitly, we introduce  $\tilde{r} = \frac{1}{r}$  and  $\tilde{t} = q^2t$  which transforms (31) into the standard BR spacetime given by

$$ds_{\pm}^2 \sim \frac{q^2}{\tilde{r}^2} \left( -d\tilde{t}^2 + d\tilde{r}^2 + \tilde{r}^2d\Omega^2 \right). \quad (32)$$

Finally, we would like to add that, in the limit  $q = 0$ , we get  $\phi = 0$ ,  $W_S = 1$ ,  $R(r) = r$ , and  $f_{\pm}(r) = 1$  which is the Minkowski flat spacetime. This indicates that the solutions are massless.

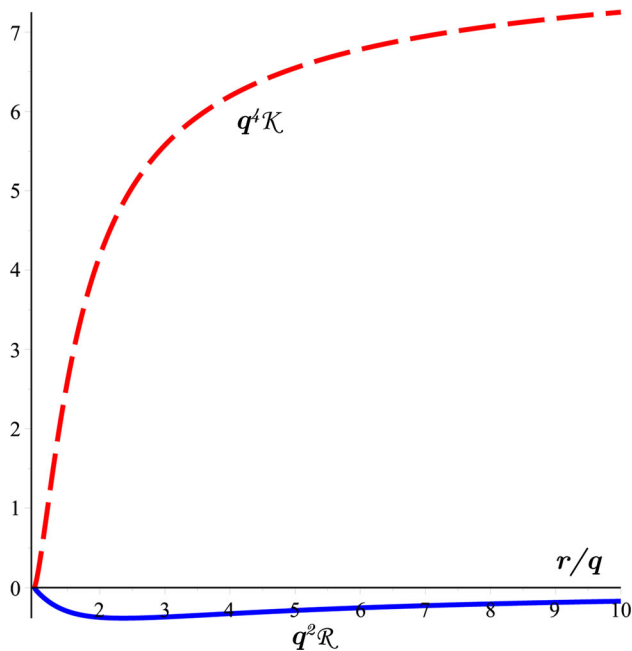


**Fig. 4** Plots of the Ricci (blue-solid) and Kretschmann (red-dash) scalars with respect to  $r/|q| \geq 1$  for the negative-branch solution. Both are zero at  $r = |q|$  and regular for  $r/|q| \geq 1$

### 3.1 The negative branch

In  $\{t, r, \theta, \varphi\}$  coordinates system the negative branch admits a physically unacceptable solution for  $r < |q|$ , which suggests imposing the constraint  $r \in [|q|, \infty)$ . For  $r \geq |q|$  the solution admits no singularity. This can be seen from the invariants of the spacetime such as the Ricci and the Kretschmann scalars which are given by

$$\mathcal{R} = \frac{2q^2}{r^4 \ln^3\left(1 - \frac{|q|}{r}\right)} \quad (33)$$

and

$$\begin{aligned} \mathcal{K} = & \frac{4q^2(12r^2 - 24|q|r + 14q^2)}{r^8 \ln^4\left(1 - \frac{|q|}{r}\right)} - \frac{4q^2(24r^2 - 64|q|r + 46q^2)}{r^8 \ln^5\left(1 - \frac{|q|}{r}\right)} \\ & + \frac{4q^2(12r^2 - 64|q|r + 67q^2)}{r^8 \ln^6\left(1 - \frac{|q|}{r}\right)} + \frac{4q^2(24|q|r - 46q^2)}{r^8 \ln^7\left(1 - \frac{|q|}{r}\right)} \\ & + \frac{56q^4}{r^8 \ln^8\left(1 - \frac{|q|}{r}\right)}, \end{aligned} \quad (34)$$

respectively. We note that,  $\lim_{r \rightarrow |q|} \mathcal{R} = 0$  and  $\lim_{r \rightarrow |q|} \mathcal{K} = 0$  while  $\lim_{r \rightarrow \infty} \mathcal{R} = 0$  and  $\lim_{r \rightarrow \infty} \mathcal{K} = \frac{8}{q^4}$ . In Fig. 4 we plot  $q^2\mathcal{R}$  and  $q^4\mathcal{K}$  in terms of  $\frac{r}{|q|}$  which are regular everywhere.

Next, to discover the wormhole properties of the solution we apply the following two successive transformations. First, we introduce  $\varrho = r - |q|$  to transform the line element of the

negative branch spacetime to an isotropic form expressed by

$$ds_-^2 = -\frac{\left(1 + \frac{|q|}{\varrho}\right)^2}{\ln^2\left(1 + \frac{|q|}{\varrho}\right)} dt^2 + \left(1 + \frac{|q|}{\varrho}\right)^2 \ln^2 \times \left(1 + \frac{|q|}{\varrho}\right) \left(d\varrho^2 + \varrho^2 d\Omega^2\right) \tag{35}$$

where  $\varrho \in [0, \infty)$ . Then we make the second coordinate transformation

$$\left(1 + \frac{|q|}{\varrho}\right) \ln\left(1 + \frac{|q|}{\varrho}\right) \varrho = r_s, \tag{36}$$

in order to go to the so-called Schwarzschild curvature coordinates where the line element reads

$$ds_-^2 = -\frac{\varrho^2 \left(1 + \frac{|q|}{\varrho}\right)^4}{r_s^2} dt^2 + \frac{1}{\left(\frac{|q|}{r_s} - \frac{1}{1 + \frac{|q|}{\varrho}}\right)^2} dr_s^2 + r_s^2 d\Omega^2. \tag{37}$$

Herein,  $\varrho$  is an implicit function of  $r_s$  with  $r_s \in [|q|, \infty)$ . To show that this spacetime represents a traversable wormhole we compare it with the standard wormhole line element

$$ds_-^2 = -e^{2\Phi(r_s)} dt^2 + \frac{1}{1 - \frac{b(r_s)}{r_s}} dr_s^2 + r_s^2 d\Omega^2 \tag{38}$$

with a throat at  $r_s = |q|$ . The red-shift function  $\Phi(r_s)$  and the shape functions  $b(r_s)$  are found to be

$$e^{2\Phi(r_s)} = \frac{\varrho^2 \left(1 + \frac{|q|}{\varrho}\right)^4}{r_s^2} \tag{39}$$

and

$$b(r_s) = r_s \left[ 1 - \left(\frac{|q|}{r_s} - \frac{1}{1 + \frac{|q|}{\varrho}}\right)^2 \right]. \tag{40}$$

First of all, in this new coordinate system i.e.,  $\{t, r_s, \theta, \varphi\}$  there is no horizon since  $e^{2\Phi(r_s)} > 0$ . In Fig. 5 we plot implicitly  $e^{2\Phi(r_s)}$  with respect to  $\frac{r_s}{|q|}$  which confirms our claim on the definite positiveness of  $e^{2\Phi(r_s)}$ .

In addition to that, in Fig. 6 we plot  $1 - \frac{b(r_s)}{r_s}$  versus  $\frac{r_s}{|q|}$  which is zero at  $r_s = |q|$  and positive afterward.

Finally we check the so called “flare-out conditions” to make sure the line element (37) is actually a traversable wormhole. The first flare-out condition implies

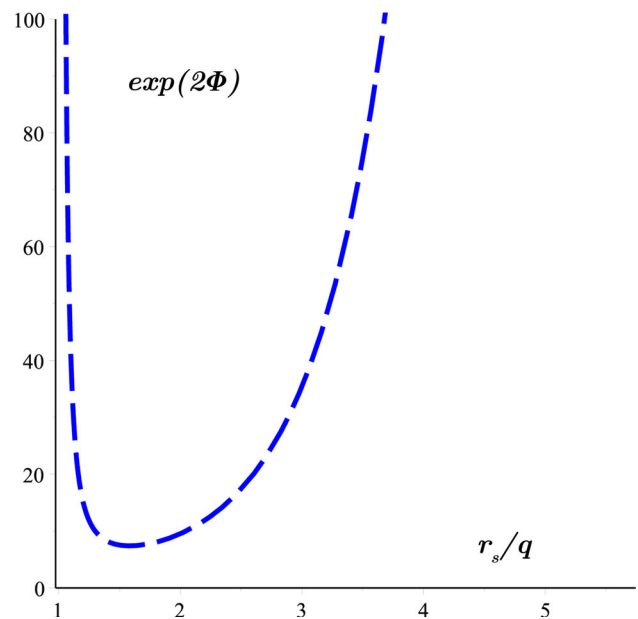


Fig. 5 Implicit plot of  $e^{2\Phi}$  in terms of  $\frac{r_s}{|q|}$  which is definite positive without a horizon

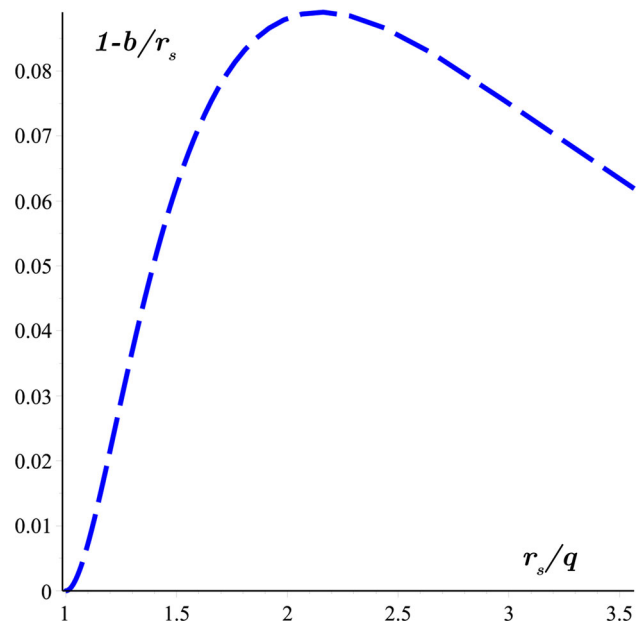


Fig. 6 Implicit plot of  $1 - \frac{b}{r_s}$  in terms of  $\frac{r_s}{|q|}$ . The graph shows that  $1 - \frac{b}{r_s}$  is definite positive for  $r_s > |q|$  and zero exactly at  $r_s = |q|$  which is the throat of the wormhole

$$b(|q|) = |q| \tag{41}$$

where  $r_s = |q|$  is the radius of the throat. Based on Fig. 6 where  $1 - \frac{b(r_s)}{r_s}$  is zero with  $\frac{r_s}{|q|} = 1$  this condition is trivially satisfied. The second flare-out condition states that

$$\frac{r_s}{b(r_s)} - 1 > 0 \tag{42}$$

for  $r_s \geq |q|$ . This condition is also satisfied considering the fact that  $1 - \frac{b}{r_s} = \left(\frac{|q|}{r_s} - \frac{1}{1 + \frac{|q|}{r_s}}\right)^2 > 0$  and consequently  $b(r_s) < r_s$  (see Fig. 6). The last flare-out condition implies  $b'(r_s) \leq \frac{b(r_s)}{r_s}$  for  $r_s \geq |q|$ .

In Fig. 7 we plot implicitly  $\frac{b(r_s) - b'(r_s)}{|q|}$  in terms of  $\frac{r_s}{|q|}$ . It implies that the last flare-out condition is satisfied locally (at and near the throat). Therefore the line element (37) is actually a wormhole with a throat located at  $r_s = |q|$ .

### 3.2 The positive branch solution

The positive branch is a naked singular solution with no horizon. The Ricci scalar is found to be

$$\mathcal{R} = \frac{2q^2}{r^4 \ln^3\left(1 + \frac{|q|}{r}\right)} \tag{43}$$

such that  $\lim_{r \rightarrow 0} R = \infty$  and  $\lim_{r \rightarrow \infty} R = 0$ . Also the Kretschmann scalar is obtained to be

$$\begin{aligned} \mathcal{K} = & \frac{4q^2(12r^2 + 24|q|r + 14q^2)}{r^8 \ln^4\left(1 + \frac{|q|}{r}\right)} - \frac{4q^2(24r^2 + 64|q|r + 46q^2)}{r^8 \ln^5\left(1 + \frac{|q|}{r}\right)} \\ & + \frac{4q^2(12r^2 + 64|q|r + 67q^2)}{r^8 \ln^6\left(1 + \frac{|q|}{r}\right)} - \frac{4q^2(24|q|r + 46q^2)}{r^8 \ln^7\left(1 + \frac{|q|}{r}\right)} \\ & + \frac{56q^4}{r^8 \ln^8\left(1 + \frac{|q|}{r}\right)}, \end{aligned} \tag{44}$$

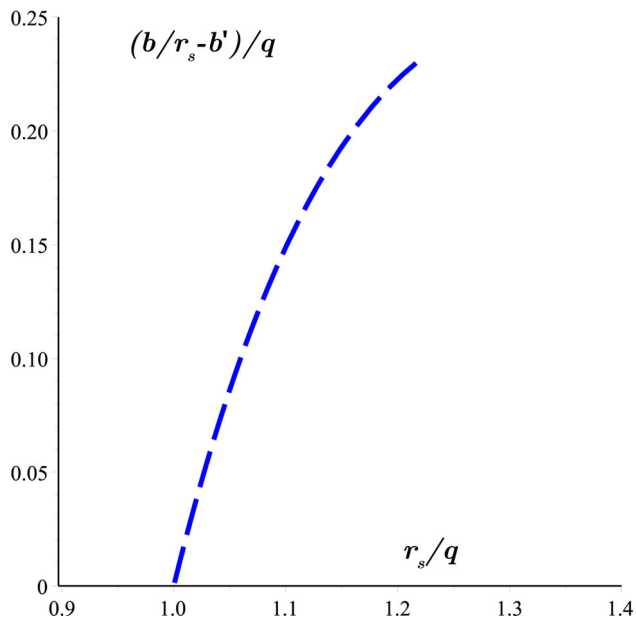


**Fig. 7** Implicit plot of  $\frac{b(r_s) - b'(r_s)}{|q|}$  in terms of  $\frac{r_s}{|q|}$ . At the throat where  $r_s = |q|$  and its vicinity  $\frac{b(r_s) - b'(r_s)}{|q|} \geq 0$

which gives  $\lim_{r \rightarrow 0} \mathcal{K} = \infty$  and  $\lim_{r \rightarrow \infty} \mathcal{K} = \frac{8}{q^4}$ . In the coordinates system  $\{t, r, \theta, \varphi\}$  the singularity is located at the origin where the invariants of the spacetime diverge.

In Fig. 8 we plot  $q^2 \mathcal{R}$  and  $q^4 \mathcal{K}$  in terms of  $\frac{r}{|q|}$ , which are both singular at  $r = 0$ . Unlike for the negative branch, the coordinate system  $\{t, r, \theta, \varphi\}$  is an appropriate system to express the positive branch solution. As we have mentioned before, asymptotically (i.e.,  $r \rightarrow \infty$ ) the positive branch line element is a charged BR spacetime. The behavior of the area of the spherical surfaces of the constant  $r$  coordinate also is remarkable. One finds

$$\mathcal{A}_+ = 4\pi R^2 = 4\pi r^2 \ln^2\left(1 + \frac{|q|}{r}\right) \tag{45}$$

such that  $\lim_{r \rightarrow 0} \mathcal{A}_+ = 0$  and  $\lim_{r \rightarrow \infty} \mathcal{A}_+ = 4\pi q^2$  and its derivative also is zero only at  $r = 0$  and  $r = \infty$ . Having asymptotically constant surface area is due to its BR-asymptotic behavior.

### 3.3 Energy–momentum tensor

Due to the hybrid form of the metric tensor for the negative branch solution in  $\{t, r_s, \theta, \varphi\}$  coordinates system we prefer to calculate the energy–momentum tensor of both solutions in the original coordinates i.e.,  $\{t, r, \theta, \varphi\}$ . The energy–momentum tensor for both cases are given by

$$T_{\mu}^{\nu} = \text{diag}[-\rho, p_r, p_{\theta}, p_{\varphi}] \tag{46}$$

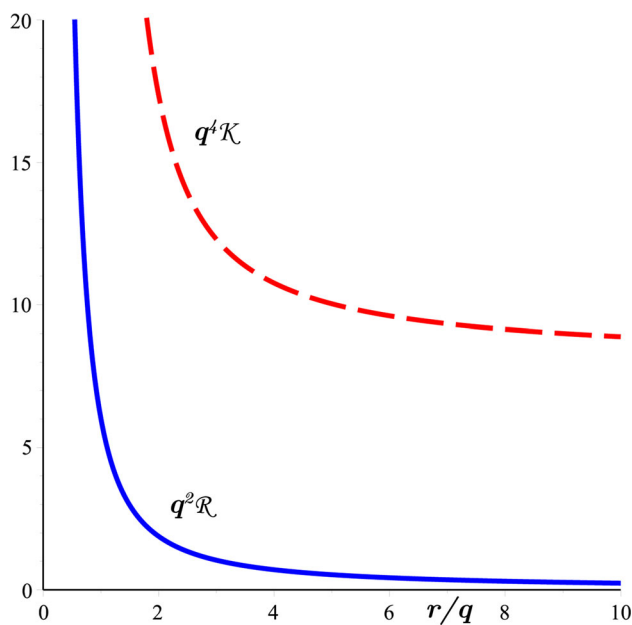


**Fig. 8** Plots of the Ricci (blue-solid) and Kretschmann (red-dash) scalars with respect to  $r/|q| \geq 1$  for the positive-branch solution. At  $r = 0$  the spacetime is singular

in which the energy density is obtained to be

$$\rho = \frac{q^2}{r^4} \frac{1 + \ln^2\left(1 \pm \frac{|q|}{r}\right)}{\ln^4\left(1 \pm \frac{|q|}{r}\right)} \tag{47}$$

and the radial and angular pressures are found as

$$-p_r = p_\theta = p_\phi = \rho - \frac{2q^2}{r^4} \frac{\ln\left(1 \pm \frac{|q|}{r}\right)}{\ln^4\left(1 \pm \frac{|q|}{r}\right)}. \tag{48}$$

The large  $r$  behavior of the energy–momentum tensor agrees with the large  $r$  behavior of the line element which we have already discussed to be of the form of the charged BR spacetime. Here we see that,

$$\lim_{r \rightarrow \infty} T_\mu^\nu = \text{diag}\left[-\frac{1}{q^2}, -\frac{1}{q^2}, \frac{1}{q^2}, \frac{1}{q^2}\right] \tag{49}$$

which is the energy–momentum tensor of the charged BR spacetime.

It is observed that, the energy conditions including Null (i.e.,  $\rho + p_i \geq 0$ ), Weak (i.e.,  $\rho \geq 0$  and  $\rho + p_i \geq 0$ ), Strong ( $\rho + \sum_{i=1}^3 p_i \geq 0$ ) and Dominant ( $\rho - |p_i| \geq 0$ ) are all satisfied for the positive branch solution. However, non of the energy conditions are satisfied for the negative branch solution. This is mostly due to the fact that in the negative branch,  $\rho + p_i < 0$ . Violation of the null-energy conditions for the wormhole spacetime is expected. This clearly shows that the wormhole is supported with exotic matter. To ensure the presence of exotic fluid near the wormhole’s throat we use the so-called the “exocity parameter” introduced as [50,51]

$$\Omega = \frac{-\rho - p_r}{|\rho|}. \tag{50}$$

If  $\Omega > 0$  then exotic matter is present at wherever it is evaluated. In our case

$$\Omega = -\frac{2q^2}{\ln^3\left(1 - \frac{|q|}{r}\right)r^4} \left| \frac{q^2}{r^4} \frac{1 + \ln^2\left(1 - \frac{|q|}{r}\right)}{\ln^4\left(1 - \frac{|q|}{r}\right)} \right|^{-1} \tag{51}$$

that is definitely positive for  $r \geq |q|$  which implies the presence of exotic matter. On the other hand, we may calculate the total amount of exotic matter by employing the Volume Integral Quantifier (VIQ) [52,53] which is given by

$$I_V = \int_{|q|}^\infty (\rho + p_r) dV. \tag{52}$$

For the wormhole solution in this study the total amount of exotic matter which violates the energy conditions is found to be

$$I_V = 8\pi q^2 \int_{|q|}^\infty \frac{dr}{r^2 \ln\left(1 - \frac{|q|}{r}\right)} \tag{53}$$

which is infinite.

### 3.4 Connection with the Einstein–Maxwell-Dilaton theory

The negative branch solution seems to be the missing chain in the black hole solution of the Einstein–Maxwell-Dilaton theory. To see this we recall that the solutions of the field equations when

$$W_D(\phi) = e^{-2\alpha\phi} \tag{54}$$

with  $\alpha$  an arbitrary dilaton parameter, are known to be

$$ds^2 = -\left(1 - \frac{r_+}{r}\right)\left(1 - \frac{r_-}{r}\right)^{\frac{1-\alpha^2}{1+\alpha^2}} dt^2 + \frac{dr^2}{\left(1 - \frac{r_+}{r}\right)\left(1 - \frac{r_-}{r}\right)^{\frac{1-\alpha^2}{1+\alpha^2}}} + r^2 \left(1 - \frac{r_-}{r}\right)^{\frac{2\alpha^2}{1+\alpha^2}} d\Omega^2 \tag{55}$$

with

$$e^{2\alpha\phi} = \left(1 - \frac{r_-}{r}\right)^{\frac{2\alpha}{1+\alpha^2}} \tag{56}$$

and

$$r_+ r_- = (1 + \alpha^2) Q^2. \tag{57}$$

We observe that the function of  $R(r) = r\left(1 - \frac{r_-}{r}\right)^{\frac{\alpha^2}{1+\alpha^2}}$  in this theory doesn’t cover its natural member i.e.,  $R(r) = r \ln\left(1 - \frac{r_-}{r}\right)$ . With the solution we presented in this study, it is now clear why  $R(r) = r \ln\left(1 - \frac{r_-}{r}\right)$  is missing. In fact, this solution is not compatible with the standard dilatonic coupling function (54), and instead, it is the solution with the coupling function given in (2). We compared the behavior of the two coupling functions in terms of the dilaton/scalar field  $\phi$  in Fig. 1.

### 4 Conclusion

We obtained an exact wormhole solution in the context of Einstein–Maxwell-Scalar gravity. The coupling function is of the *Subclass IIA or scalarised-connected-type* in accordance with the classification in Ref. [38]. Our coupling function i.e.,  $W_S(\phi) = \frac{16}{\phi^4 - 4\phi^2 + 16}$  is a new Mexican hat-type potential with two maximum at  $\phi = \pm\sqrt{2}$  and one minimum at  $\phi = 0$  and also  $W_S(\phi)$  asymptotically goes to zero. The solution admits two branches namely the positive and the negative one. The positive branch is a non-black hole singular cosmological object which asymptotically goes to the well-known charged BR metric. On the other hand, the negative branch is a wormhole solution supported by infinite exotic matter. In the former case the radial coordinate  $r \in [0, \infty)$ , however in the later case  $r \in [|q|, \infty)$  where  $q$  stands for the electric charge. In the negative branch solution, to reveal it is a wormhole we have transformed the solution from  $\{t, r, \theta, \phi\}$  to the Schwarzschild curvature coordinates  $\{t, r_s, \theta, \varphi\}$  where

we have shown that all flare-out conditions are satisfied. Here when the charge is zero the entire theory reduces to the vacuum flat Minkowski spacetime. This feature in the negative branch reminds us of the charged Einstein–Rosen bridge [3] (quasi-charged bridge) where Einstein and Rosen set the mass of the Reissner–Nordström to be zero and the charge to be pure imaginary (a non-physical assumption). Here, in comparison, we ask: whether the negative branch is a naturally charged Einstein–Rosen bridge? This needs more investigation which we conduct in a separate work.

**Data Availability Statement** This manuscript has no associated data or the data will not be deposited. [Authors' comment: This theoretical work does not use or produce numerical data.]

**Open Access** This article is licensed under a Creative Commons Attribution 4.0 International License, which permits use, sharing, adaptation, distribution and reproduction in any medium or format, as long as you give appropriate credit to the original author(s) and the source, provide a link to the Creative Commons licence, and indicate if changes were made. The images or other third party material in this article are included in the article's Creative Commons licence, unless indicated otherwise in a credit line to the material. If material is not included in the article's Creative Commons licence and your intended use is not permitted by statutory regulation or exceeds the permitted use, you will need to obtain permission directly from the copyright holder. To view a copy of this licence, visit <http://creativecommons.org/licenses/by/4.0/>.

Funded by SCOAP<sup>3</sup>.

## References

1. L. Flamm, Phys. Z. **17**, 448 (1916)
2. K. Schwarzschild, Sitzungsberichte der Königlich Preussischen Akademie der Wissenschaften. **7**, 189 (1916)
3. A. Einstein, N. Rosen, Phys. Rev. **48**, 73 (1935)
4. M.S. Morris, K.S. Thorne, Am. J. Phys. **56**, 395 (1988)
5. M. Visser, *Lorentzian Wormholes: From Einstein To Hawking* (American Institute of Physics Press, New York, 1996)
6. F.S.N. Lobo, M.A. Oliveira, Phys. Rev. D **80**, 104012 (2009)
7. O. Sokoliuk, A. Baransky, Eur. Phys. J. C **81**, 781 (2021)
8. A. Banerjee, A. Pradhan, T. Tangphati, F. Rahaman, Eur. Phys. J. C **81**, 1031 (2021)
9. F.S.N. Lobo, Int. J. Mod. Phys. D **25**, 1630017 (2016)
10. M.B. Green, J.H. Schwarz, E. Witten, *Superstring Theory* (Cambridge University Press, Cambridge, 1987)
11. D. Garfinkle, G. Horowitz, A. Strominger, Phys. Rev. D **43**, 3140 (1991)
12. D. Brill, G. Horowitz, Phys. Lett. B **262**, 437 (1991)
13. R. Gregory, J. Harvey, Phys. Rev. D **47**, 2411 (1993)
14. T. Koikawa, M. Yoshimura, Phys. Lett. B **189**, 29 (1987)
15. D. Boulware, S. Deser, Phys. Lett. B **175**, 409 (1986)
16. M. Rakhmanov, Phys. Rev. D **50**, 5155 (1994)
17. B. Harms, Y. Leblanc, Phys. Rev. D **46**, 2334 (1992)
18. C.F.E. Holzhey, F. Wilczek, Nucl. Phys. B **380**, 447 (1992)
19. G.W. Gibbons, Nucl. Phys. B **207**, 337 (1982)
20. I.Z. Fisher, Zh. Eksp. Teor. Fiz. **18**, 636 (1948)
21. D. Garfinkle, G.T. Horowitz, A. Strominger, Phys. Rev. D **43**, 3140 (1991)
22. K.C.K. Chan, J.H. Horne, R.B. Mann, Nucl. Phys. B **447**, 441 (1995)
23. G. Clement, C. Leygnac, Phys. Rev. D **70**, 084018 (2004)
24. R.-G. Cai, A.Z. Wang, Phys. Rev. D **70**, 084042 (2004)
25. A. Sheykhi, M.H. Dehghani, N. Riazi, Phys. Rev. D **75**, 044020 (2007)
26. S.H. Hendi, J. Math. Phys. **49**, 082501 (2008)
27. S. Yu, J. Qiu, G. Changjun, Class. Quantum Gravity **38**, 105006 (2021)
28. J. Qiu, Eur. Phys. J. C **81**, 1094 (2021)
29. M.M. Akbar, E. Woolgar, Class. Quantum Gravity **26**, 055015 (2009)
30. C.A.R. Herdeiro, E. Radu, N. Sanchis-Gual, J.A. Font, Phys. Rev. Lett. **121**, 101102 (2018)
31. Z.-Y. Fan, H. Lü, JHEP **09**, 060 (2015)
32. F. Yao, Eur. Phys. J. C **81**, 1009 (2021)
33. Y.S. Myung, D.-C. Zou, Eur. Phys. J. C **79**, 273 (2019)
34. Y.S. Myung, C. Zou, Eur. Phys. J. C **79**, 641 (2019)
35. C.A.R. Herdeiro, J.M.S. Oliveira, E. Radu, Eur. Phys. J. C **80**, 23 (2020)
36. G. Guoa, P. Wangb, H. Wuc, H. Yang, Eur. Phys. J. C **81**, 864 (2021)
37. P. Kanti, B. Kleihaus, J. Kunz, Phys. Rev. Lett. **107**, 271101 (2011)
38. D. Astefanesei, C. Herdeiro, A. Pombod, E. Radu, JHEP **10**, 078 (2019)
39. R. Ibadov, B. Kleihaus, J. Kunz, S. Murodov, Symmetry **13**, 89 (2021)
40. D.D. Doneva, S.S. Yazadjiev, Phys. Rev. Lett. **120**, 131103 (2018)
41. H.O. Silva, J. Sakstein, L. Gualtieri, T.P. Sotiriou, E. Berti, Phys. Rev. Lett. **120**, 131104 (2018)
42. G. Antoniou, A. Bakopoulos, P. Kanti, Phys. Rev. Lett. **120**, 131102 (2018)
43. P.V. Cunha, C.A. Herdeiro, E. Radu, Phys. Rev. Lett. **123**, 011101 (2019)
44. Y.S. Myung, D.-C. Zou, Phys. Lett. B **814**, 136081 (2021)
45. D.-C. Zou, Y.S. Myung, Phys. Lett. B **820**, 136545 (2021)
46. S.-J. Zhang, Eur. Phys. J. C **81**, 441 (2021)
47. B. Bertotti, Phys. Rev. **116**, 1331 (1959)
48. I. Robinson, Bull. Akad. Pol. **7**, 351 (1959)
49. D. Garfinkle, E.N. Glass, Class. Quantum Gravity **28**, 215012 (2011)
50. M. Visser, *Lorentzian Wormholes: From Einstein to Hawking*. Matt Visser (Washington U., St. Louis., 1995). ISBN:9781563966538
51. S. Capozziello, M. De Laurentis, S.D. Odintsov, A. Stabile, Phys. Rev. D **83**, 064004 (2011)
52. M. Visser, S. Kar, N. Dadhich, Phys. Rev. Lett. **90**, 201102 (2003)
53. S. Kar, N. Dadhich, M. Visser, Pramana **63**, 859–864 (2004)